

Identifying the Neutrino mass Ordering with INO and NOvA

Mattias Blennow^{*}, Thomas Schwetz[†],

Max-Planck-Institut für Kernphysik, Saupfercheckweg 1, 69117 Heidelberg, Germany

Abstract

The relatively large value of θ_{13} established recently by the Daya Bay reactor experiment opens the possibility to determine the neutrino mass ordering with experiments currently under construction. We investigate synergies between the NOvA long-baseline accelerator experiment with atmospheric neutrino data from the India-based Neutrino Observatory (INO). We identify the requirements on energy and direction reconstruction and detector mass for INO necessary for a significant sensitivity. If neutrino energy and direction reconstruction at the level of 10% and 10° can be achieved by INO a determination of the neutrino mass ordering seems possible around 2020.

arXiv:1203.3388v3 [hep-ph] 24 Oct 2012

^{*}blennow AT mpi-hd.mpg.de

[†]schwetz AT mpi-hd.mpg.de

1 Introduction

Huge progress has been achieved in the study of neutrino oscillations [1–5] and a rough picture of the structure of three-flavour lepton mixing has been obtained, with two large mixing angles (θ_{12} and θ_{23}) and two neutrino mass-squared differences separated roughly by a factor 30: $\Delta m_{21}^2 \simeq 7.6 \cdot 10^{-5} \text{ eV}^2$ and $|\Delta m_{31}^2| \simeq 2.4 \cdot 10^{-3} \text{ eV}^2$, see [6, 7] for a recent global fit. The sign of Δm_{21}^2 is determined by the matter effect [8–10] inside the sun being responsible for the flavour transition of solar neutrinos.¹ In contrast the sign of Δm_{31}^2 is not known and present data cannot distinguish between the so-called normal or inverted neutrino mass ordering, with $\Delta m_{31}^2 > 0$ or $\Delta m_{31}^2 < 0$, respectively. The determination of the sign of Δm_{31}^2 is one of the most important goals of the future neutrino oscillation program. The type of the neutrino mass ordering provides crucial information on the flavour structure in the lepton sector. Furthermore, the unknown sign of Δm_{31}^2 introduces a two-fold ambiguity in the determination of the parameters θ_{13} and δ by long-baseline experiments [11, 12], and might severely affect the search for CP violation in neutrino oscillations.

The most promising way to determine the neutrino mass ordering is to search for matter effects [8–10] in oscillations driven by Δm_{31}^2 . This requires the participation of the electron neutrino in such oscillations, which is suppressed by the mixing angle θ_{13} . Therefore, the size of θ_{13} strongly affects the possibility to determine the sign of Δm_{31}^2 . Recently the Daya Bay reactor neutrino experiment established a non-zero value of θ_{13} at the 5σ level [13],

$$\sin^2 2\theta_{13} = 0.092 \pm 0.016(\text{stat}) \pm 0.005(\text{syst}). \quad (1)$$

A similar result was later found also by the RENO experiment [14]

$$\sin^2 2\theta_{13} = 0.113 \pm 0.013(\text{stat}) \pm 0.019(\text{syst}). \quad (2)$$

These results confirm previous hints for a relatively large value of θ_{13} from the T2K [15] and Double Chooz [16] experiments, see also [7]. Given these exciting developments, the question arises whether there is a chance to determine the neutrino mass ordering with currently running or planned experiments. This possibility will have an important impact on the planning and design of a subsequent generation of oscillation experiments towards the search for leptonic CP violation.

The main goal of the current generation of accelerator experiments (T2K [17] and NOvA [18]) as well as reactor experiments (Double-Chooz [19], RENO [20], and Daya Bay [21]) is the determination of θ_{13} , see [22] for a recent review. From those experiments only NOvA may have sensitivity to the sign of Δm_{31}^2 . However, the study performed in [23] shows that, combining expected data from NOvA with the ones from all the other

¹The convention-independent statement is that the neutrino mass state which contains dominantly the electron neutrino (denoted by ν_1 per convention) has to be the lighter of the two mass states responsible for the flavour transitions observed for solar neutrinos and reactor anti-neutrinos in the KamLAND experiment.

mentioned experiments, only a poor sensitivity to the neutrino mass ordering will be obtained: for $\sin^2 2\theta_{13} \approx 0.09$ the sign of Δm_{31}^2 can be determined at 90% CL in 2019 only for about 45% of all possible values of the CP phase δ and there is negligible sensitivity at higher CL. Even for a fully optimised run time schedule as well as optimistic upgrade assumptions for T2K and NOvA, the global data from those experiments extrapolated until 2025 will provide sensitivity at 3σ for only about 35% of all δ values. For similar studies see also [24–26].

Motivated by this situation we explore here the possibility to use data from atmospheric neutrinos in order to determine the mass ordering. In particular, in the India-based Neutrino Observatory (INO) [27] a magnetized iron calorimeter will be built for the observation of charge separated muons induced from atmospheric neutrinos, with a 50 kt detector expected to start data taking in 2017 [28]. A comparable small sample of such atmospheric neutrino events has been observed by the MINOS detector [29,30]. For large enough values of θ_{13} matter effects will induce characteristic signatures for atmospheric muon neutrinos as a function of the neutrino energy and zenith angle, different for neutrinos and anti-neutrinos, depending on the mass ordering, due to three-flavour matter effects [31–34], see also [35]. The sensitivity of magnetized iron detectors to those effects has been studied in [36–44]. Also non-magnetized atmospheric neutrino detectors may provide sensitivity to the neutrino mass ordering, see e.g., [43,45–50]. However, the lack of event-by-event discrimination of neutrino and anti-neutrino induced events leads to a dilution of the relevant signatures and therefore huge detectors will be required [51,52].

In the following we will investigate the impact of the INO atmospheric neutrino data on the sensitivity to the neutrino mass ordering in a global context by combining simulated data from INO, NOvA, and T2K. The remainder of this work is organized as follows. In section 2 we give details of our simulation of atmospheric and accelerator data, as well as on the statistical analysis. The main results are presented in section 3, where we discuss the combined sensitivity of atmospheric and accelerator data as a function of time for various assumptions on the experimental configuration achieved in INO. In section 4 we discuss the effect of neglecting the solar mass-squared difference Δm_{21}^2 in the INO analysis. We conclude in section 5.

2 Simulation details

2.1 Atmospheric neutrinos in INO

For the simulation of atmospheric data in INO we follow closely [40], where technical details for the calculation of the event rates, the used cross section and neutrino fluxes, as well as the statistical analysis are given. Here we summarize our main assumptions. We assume a muon threshold of 2 GeV and assume that muon charge identification is perfect with an efficiency of 85% above that threshold. As stressed in [39,40] the energy and direction reconstruction resolutions are crucial parameters for the sensitivity to the

mass ordering. The ability to reconstruct neutrino energy and direction depends on the corresponding resolutions for the muon, the mean angle between muon and neutrino, and the energy and momentum reconstruction for the hadronic shower. In the absence of detailed Monte Carlo simulations we assume that neutrino energy and direction resolutions are Gaussian with widths σ_E and σ_θ , respectively, assuming two representative sets of values, corresponding to a “low” or “high” resolution configuration:

$$\begin{aligned}\sigma_E/E_\nu &= 0.15, & \sigma_\theta &= 15^\circ & (\text{low}) \\ \sigma_E/E_\nu &= 0.10, & \sigma_\theta &= 10^\circ & (\text{high})\end{aligned}\tag{3}$$

We take those resolutions to be independent of energy or zenith angle. In a real experiment neither the resolutions nor charge ID efficiencies will be constant, and one may expect different data samples with diverse reconstruction qualities. Unfortunately detailed reconstruction capabilities of the INO detector are currently not available. Therefore we make the simplified assumptions stated above. Our results should be considered as a representative estimate assuming that the adopted values can be achieved in average for the majority of the events. With a constant efficiency of 85% and a muon threshold of 2 GeV we find 242 (223) μ -like events per 50 kt yr exposure for the high (low) resolution assuming no oscillations (sum of neutrino and anti-neutrino events).

As shown in [40] e -like events provide additional sensitivity to the mass ordering. However, electrons and positrons induce electromagnetic showers in an INO-like detector and the reconstruction and charge separation of such events is difficult. Currently it is not foreseen to consider e -like events in INO. Therefore we do not include them in our analysis.

We divide the simulated data into 20 bins in reconstructed neutrino energy from 2 GeV to 10 GeV, as well as 20 bins in reconstructed zenith angle from $\cos\theta = -1$ to $\cos\theta = -0.1$. We then fit the two-dimensional event distribution in the 20×20 bins by using the appropriate χ^2 -definition for Poisson distributed data, while also including the following systematic uncertainties: we assume a 20% uncertainty on the over-all normalization of events, and 5% on each of the neutrino/anti-neutrino event ratio, the ν_μ to ν_e flux ratio, the zenith-angle dependence, and on the energy dependence of the fluxes, see [40] for details.

In the simulation of atmospheric neutrino data we set $\Delta m_{21}^2 = 0$. This is a reasonable approximation for neutrino energies above 2 GeV. We estimate the accuracy of this approximation in section 4. Under this assumption, atmospheric neutrino data depend on the three parameters $\Delta m_{\text{eff}}^2, \theta_{23}, \theta_{13}$. For the NOvA and T2K simulations we use full three-flavour oscillation probabilities including Δm_{21}^2 effects. In order to combine such simulations with INO we use for the atmospheric analysis an effective mass-squared difference, which is related to Δm_{31}^2 by [53] (see also [54])

$$\Delta m_{\text{eff}}^2 = \Delta m_{31}^2 - (\cos^2 \theta_{12} - \cos \delta \sin \theta_{13} \sin 2\theta_{12} \tan \theta_{23}) \Delta m_{21}^2.\tag{4}$$

This is particularly important when investigating the sensitivity to the mass ordering,

since to very good approximation the degenerate solutions occur at $\pm\Delta m_{\text{eff}}^2$, which corresponds to slightly differing values of $|\Delta m_{31}^2|$ according to the above equation.

2.2 NOvA, T2K, and reactor experiments

For the simulation of the long-baseline accelerator experiments NOvA and T2K we use the GLoBES software [55, 56] and follow closely the analysis of [23], where details on the assumed experimental parameters can be found. For T2K, we always assume the final exposure corresponding to 5 years running with a beam power of 0.75 MW in neutrinos only. Assuming a realistic beam power evolution, such an exposure will be obtained around 2018. For NOvA, the nominal exposure is 3 years for neutrinos and anti-neutrinos each, with $6 \cdot 10^{20}$ POT per year and a 15 kt detector. When considering the time evolution of the sensitivity we assume the run plan for alternating neutrino and anti-neutrino beams as well as the time evolution of the detector mass as shown in Fig. 11 of [22]. This should be considered as one particular representative example, and in this scenario the nominal exposure would be reached around 2019 for neutrinos and 2020 for anti-neutrinos. We assume that the experiment is terminated after this date.

The main sensitivity to the mass ordering comes from NOvA due to the somewhat larger matter effect, because of the longer baseline of 810 km. The matter effect is significantly smaller in T2K (295 km baseline) and therefore T2K has no sensitivity to the mass ordering. However, T2K may contribute indirectly by providing additional information on θ_{13} and the phase δ . Therefore, we always consider the combination of both beams in the following.

We include the determination of $\sin^2 2\theta_{13}$ from reactor experiments as a simple Gaussian prior centered at 0.09 with the current Daya Bay error of 0.017 at 1σ (systematic and statistical errors combined). While improved data from the running reactor experiments will tighten these bounds, the actual sensitivity of INO and NOvA to the mass ordering does not depend crucially on the exact error.

2.3 Parameter values and implementation

For our simulations, we have fixed the values of the true neutrino oscillation parameters to

$$\begin{aligned} \Delta m_{\text{eff}}^2 &= 2.4 \cdot 10^{-3} \text{ eV}^2, \quad \Delta m_{21}^2 = 7.8 \cdot 10^{-5} \text{ eV}^2, \\ \theta_{23} &= 45^\circ, \quad \theta_{12} = 33^\circ, \quad \sin^2 2\theta_{13} = 0.09, \end{aligned} \tag{5}$$

unless stated otherwise. When treating the accelerator experiments, the sensitivity to the mass ordering depends significantly on the true values of the CP phase δ . We fix Δm_{21}^2 and θ_{12} in our fits, since the impact of these parameters is expected to be minimal. Other parameters are marginalized over, and we impose the following priors (1σ Gaussian errors): $\sigma(\sin^2 2\theta_{13}) = 0.017$ (the uncertainty from Daya Bay [13]), $\sigma(\Delta m_{31}^2) = 0.5|\Delta m_{13}^2|$ (this is a very weak prior with the only purpose to guide the minimization algorithm), and

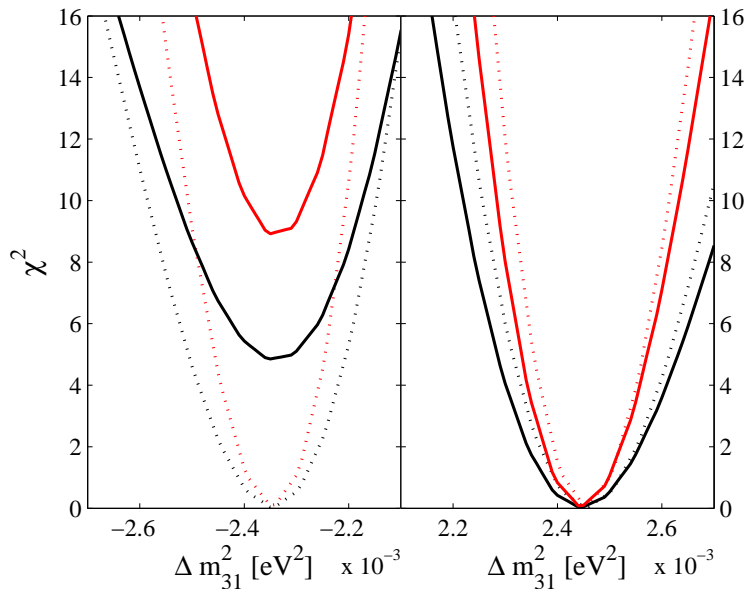


Figure 1: The dependence of the marginalized atmospheric χ^2 as a function of Δm_{31}^2 in the different mass orderings assuming $|\Delta m_{\text{eff}}^2| = 2.4 \cdot 10^{-3} \text{ eV}^2$. The dotted (solid) curves correspond to $\sin^2 2\theta_{13} = 0$ (0.09) and the black (red) curves to a detector mass of 50 kt (100 kt). The running time has been assumed to be 10 years with the high resolution scenario.

$\sigma(\theta_{23}) = 0.08\theta_{23}$. The prior on θ_{23} corresponds to $\sigma(\sin^2 \theta_{23}) \approx 0.063$ at $\theta_{23} = 45^\circ$, which is approximately the accuracy from current data [6]. Once T2K and NOvA are included in the fit, they will provide a more accurate determination of θ_{23} than this prior. By default we assume that the true mass ordering is normal and test the sensitivity to exclude the inverted ordering. With the above mentioned priors the results are very similar if the true ordering is inverted, as we will show explicitly towards the end of section 3. For each simulated value of the true parameters, we find the minimum value of the χ^2 in the opposite mass ordering. When reporting sensitivity in terms of standard deviations we use one degree of freedom to evaluate the χ^2 . Hence the number of σ with which the wrong mass ordering can be excluded is given by the square-root of the $\Delta\chi^2$ between the two signs of Δm_{31}^2 .

In Fig. 1, we show the behavior of the marginalized χ^2 as a function of Δm_{31}^2 for the case of atmospheric only for $\sin^2 2\theta_{13} = 0$ and 0.09, respectively. As can be seen from the figure, the mass orderings are indistinguishable when $\sin^2 2\theta_{13} = 0$, while there is a significant difference for $\sin^2 2\theta_{13} = 0.09$. Also note the shifts in the best fit of Δm_{31}^2 as compared to the simulated Δm_{eff}^2 , which are well in agreement with Eq. 4.

Let us stress that the sensitivity of atmospheric data on the mass ordering also depends on the value of θ_{23} , with typically improved (weaker) sensitivity for $\theta_{23} > 45^\circ$ ($< 45^\circ$). This effect has been investigated in [40]. Here we always assume a true value $\theta_{23} = 45^\circ$ in order to represent the “average” sensitivity and briefly show this behavior in the end of

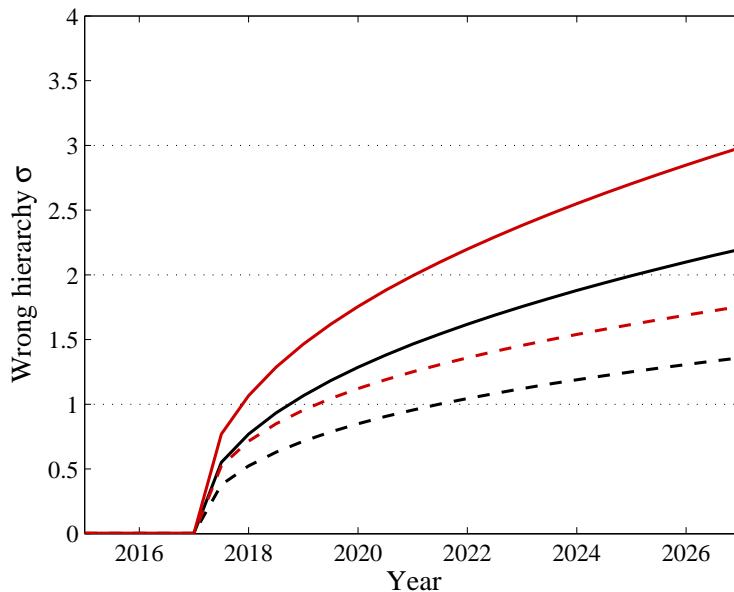


Figure 2: The sensitivity of an INO-like detector only as evolved in time assuming start of data taking in the beginning of 2017 (ticks in the figure correspond to the beginning of the year). We show the number of standard deviations with which the wrong mass ordering can be excluded. Black (red) curves correspond to a detector mass of 50 kt (100 kt) and dashed (solid) curves correspond to the low (high) resolution scenario (see text). We assume true values $\sin^2 2\theta_{13}^{\text{tr}} = 0.09$, $\theta_{23}^{\text{tr}} = \pi/4$, and impose external priors at 1σ of $\sigma(\sin^2 2\theta_{13}) = 0.017$ and $\sigma(\theta_{23}) = 0.08\theta_{23}^{\text{tr}}$.

the next section.

3 Results

Let us first investigate the sensitivity of atmospheric data alone. In Fig. 2, we show how the sensitivity of INO only to excluding the inverted ordering would evolve in time, depending on implemented scenario. We would like to remind that to a fairly good approximation this sensitivity is independent of δ and will be slightly worse if the effects of this parameter are included (see Sec. 4). From this figure, we can deduce that the sensitivity of atmospheric data would be strongly dependent on how well the atmospheric study can be performed. In particular, in comparing the best and worse cases, the high resolution 100 kt scenario would reach a 90% CL sensitivity after slightly less than two years of running, while the low resolution 50 kt scenario would not accomplish this within the assumed 10 year lifetime of the experiment, after which the high resolution 100 kt scenario has reached a sensitivity close to 3σ . Note that the high resolution 50 kt scenario outperforms the low resolution 100 kt scenario, implying that reaching for an increase in resolution may be preferable to increasing the detector mass [39, 40], depending on the

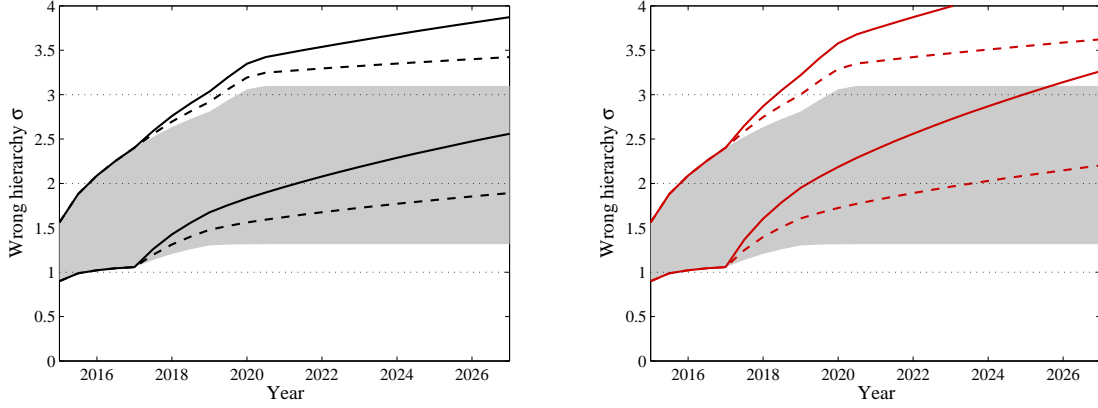


Figure 3: The minimum and maximum sensitivities (depending on the true value of δ) of atmospheric combined with NOvA and T2K. We show the number of standard deviations with which the wrong mass ordering can be excluded. The left (right) panel corresponds to a detector mass of 50 kt (100 kt) and dashed (solid) curves correspond to the low (high) resolution scenario. The shaded area is the corresponding result for NOvA and T2K only. The true value of $\sin^2 2\theta_{13}$ has been assumed to be 0.09.

cost and technical feasibility of doing so.

The sensitivity to exclude the inverted mass ordering by combining information from INO together with NOvA and T2K is presented in Fig. 3. Since the sensitivity depends on the true value of the CP violating phase δ , we show both the maximum and minimum sensitivities, corresponding to the most and least favourable values of δ , respectively. For comparison, we have also included the sensitivity of the accelerator based experiments only. The kink in the least favourable curve is due to the onset of anti-neutrino running in NOvA, which in our example time line happens simultaneously with the onset of INO data taking in 2017. From this figure, we see that in the low resolution scenarios the sensitivity to the mass ordering is mildly improved compared to that of the accelerator experiments only, increasing by roughly $0.5\sigma - 1\sigma$ after the full 10 years of running, depending on the scenario and the value of δ . For these scenarios, the atmospheric data only slightly adds information to the accelerator data during the running time of NOvA, resulting in a given sensitivity to be reached marginally ahead of when it would be reached by accelerator experiments alone.

For the higher resolution scenarios, the rise in the precision is significantly faster, in particular during the time when atmospheric and accelerator experiments are running in parallel. This results in a significant improvement in the sensitivities in a relatively short time span. It should be noted that this effect is present both for the values of δ to which accelerator experiments are most sensitive, as well as those values to which they are least sensitive, leading to an overall increase in the sensitivity irrespective of the value of δ . The statistical level where the synergy between atmospheric and accelerator experiments is most apparent is around the 2σ region for the least favourable values of δ , where the

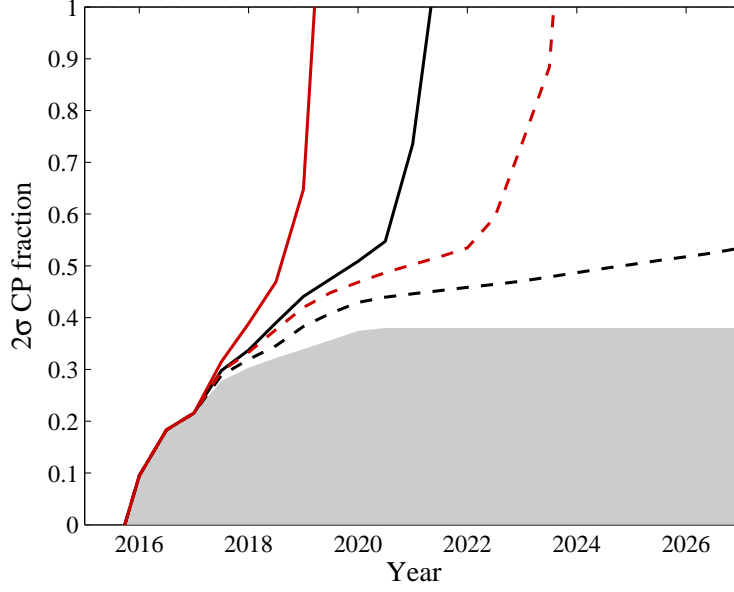


Figure 4: The time evolution of the fraction of values of the CP violating phase δ for which the combination of INO, NOvA, and T2K would be sensitive to the mass ordering at 2σ . Black (red) curves correspond to a detector mass of 50 kt (100 kt) and dashed (solid) curves correspond to the low (high) resolution scenario. The shaded area is the corresponding result for NOvA and T2K only. The true value of $\sin^2 2\theta_{13}$ has been assumed to be 0.09.

final sensitivity is impacted by both types of experiment. Most noticeably, NOvA and T2K never reach this sensitivity by themselves, while the high resolution atmospheric data by itself would reach it several years later than the combined. Most strikingly, the combined sensitivity in the most optimistic high resolution 100 kt scenario would reach the 2σ within 2 years of the start of atmospheric data taking, still within the lifetime of NOvA.

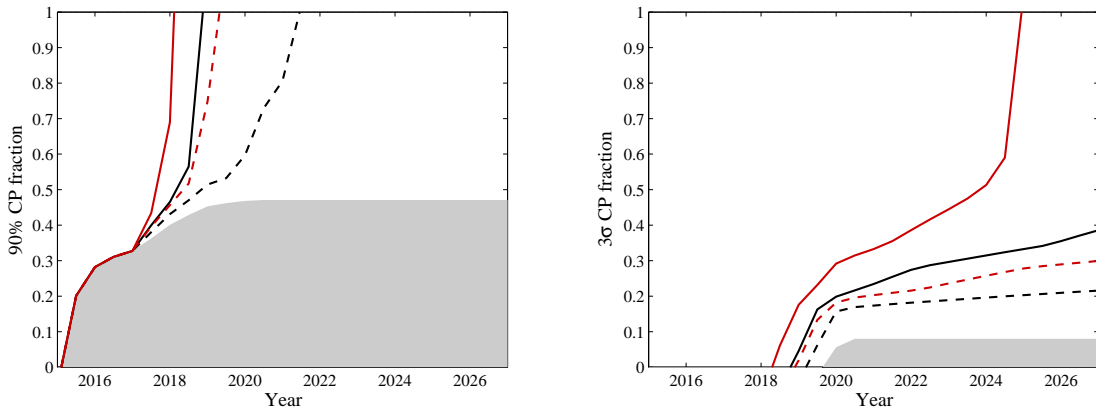


Figure 5: Same as Fig. 4 but for sensitivity at the 90% (3σ) CL for the left (right) panel.

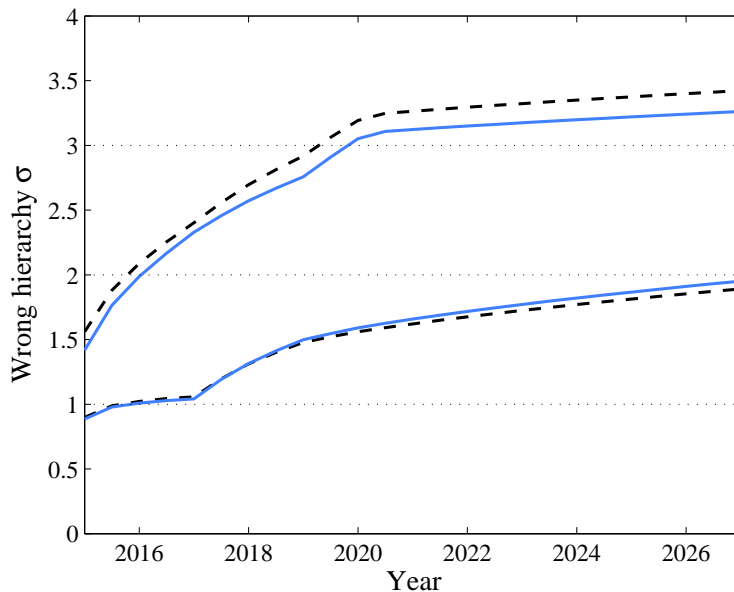


Figure 6: The minimum and maximum sensitivities (depending on the true value of δ) of atmospherics combined with NOvA and T2K assuming that the true mass ordering is normal (inverted) for dashed-black (solid-blue). We assume a detector mass of 50 kt, low resolution, and a true value $\sin^2 2\theta_{13} = 0.09$.

In Fig. 4, we show the time evolution of the 2σ CP fraction, the fraction of the values of true δ (assuming a flat distribution) for which the sensitivity to the mass ordering is 2σ or better. Note that this information is complementary to that presented in the previous figure, as it also contains information about the sensitivity dependence on δ , not just the maximum and minimum sensitivity. Comparing these two figures, we can deduce that unfortunately there are more values of δ which are close to the minimal sensitivity than to the maximal one. In particular, for the worst case of low resolution and a 50 kt detector, the 2σ CP fraction remains around 0.5 by 2027, even though the minimal sensitivity at this point is around 1.9σ . This is further illustrated by the rate at which the CP fraction grows after reaching 0.5 for the other scenarios. For completeness, we also show the 90% and 3σ CP fractions in Fig. 5. We deduce from these figures that it would be relatively easy to obtain a 90% CL hint for rejecting the inverted ordering, while a 3σ evidence will be significantly more challenging. However, in both cases, the interplay between atmospheric and accelerator data will allow for establishing these at an earlier time, regardless of the true value of δ or the confidence level in question.

So far we always assumed that the true mass ordering is normal. In Fig. 6 we compare the difference in sensitivity between a true normal or inverted mass ordering, confirming that the sensitivity is very similar. The features induced by the matter resonance will appear in the data either for neutrinos or anti-neutrinos, depending on whether the true ordering is normal or inverted, respectively. While statistics will be larger for neutrinos than for anti-neutrinos, the important quantity for the sensitivity is the *difference* in

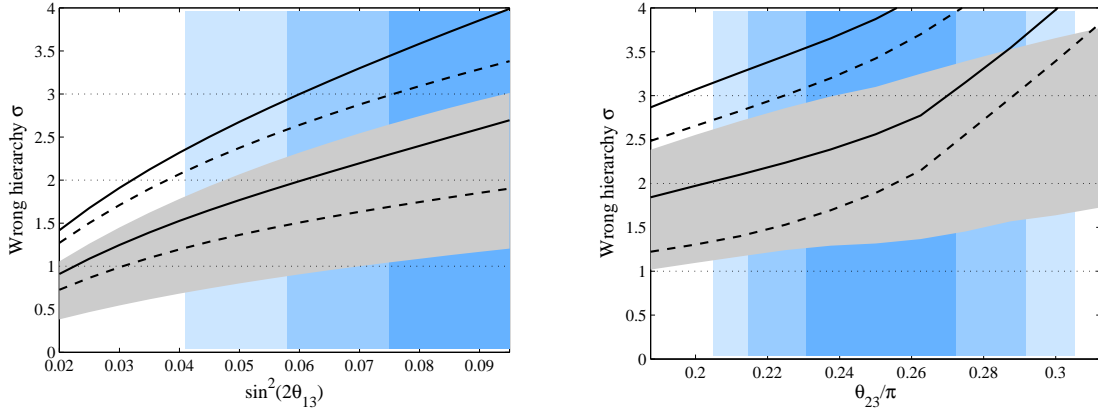


Figure 7: The minimum and maximum sensitivities (depending on the true value of δ) of atmospheric neutrinos combined with NOvA and T2K as a function of the true value of θ_{13} (left) and θ_{23} (right), respectively. We show the number of standard deviations with which the wrong mass ordering can be excluded. We have assumed the total final exposures for NOvA and T2K, and an exposure of 500 kt yr for INO. Dashed (solid) curves correspond to the low (high) resolution scenario. The gray-shaded area is the corresponding result for NOvA and T2K only. The blue-shaded areas indicate the current 1, 2, 3 σ regions of the parameters (from dark to light shading).

event numbers expected for the different mass orderings in each of the two samples, and this difference is largely independent of the true ordering. This statement is true for approximately fixed oscillation parameters, especially θ_{13} . Our simulation shows that the accuracy on θ_{13} and other parameters as provided by current Daya Bay data as well as the simulated data from T2K and NOvA, is sufficient for the above argument to be valid, in agreement with [40]. For Fig. 6 we have assumed a 50 kt detector mass and low resolution for INO. Corresponding results for all other configurations considered in this work are very similar to the one shown in Fig. 6.

Despite the strong evidence for a non-zero (and relatively large) value for θ_{13} the current uncertainty from Daya Bay [13] still allows for a significant spread in $\sin^2 2\theta_{13}$, see Eq. 1. In Fig. 7 we show the dependence of the sensitivity to the mass ordering as a function of the true value of $\sin^2 2\theta_{13}$, assuming the final exposure for all experiments. The blue shading indicates the 1, 2, and 3 σ lower bounds on $\sin^2 2\theta_{13}$ according to Eq. 1. We observe that if the true value of θ_{13} happens to be close to the current 3 σ lower bound, the sensitivity to the mass ordering will be noticeably weaker than at the current best fit point, typically allowing for an exclusion of the wrong hierarchy with about one standard deviation smaller significance. Correspondingly better sensitivities can be achieved for θ_{13} larger than the current best fit point (not shown). In a similar fashion, we also show the dependence of the sensitivity on the mixing angle θ_{23} . As shown in [40], the sensitivity becomes better for values of θ_{23} above $\pi/4$ and worse for smaller values, see e.g., Eq. 32 of [40]. It is also notable that for smaller values the atmospheric neutrinos help only marginally,

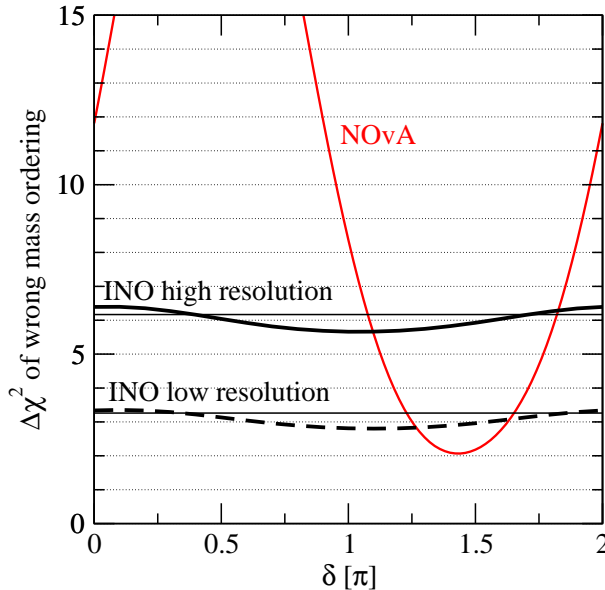


Figure 8: $\Delta\chi^2$ of the wrong mass ordering for $\sin^2 2\theta_{13} = 0.09$ including a finite Δm_{21}^2 in the INO simulation as a function of the CP phase δ . Data is simulated for normal mass ordering and $\delta = 0$. Those data are fitted assuming the inverted mass ordering varying δ . When changing the sign of Δm_{31}^2 we keep $|\Delta m_{\text{eff}}^2|$ constant, see Eq. 4, and all other oscillation parameters are fixed. For INO only statistical errors are taken into account, corresponding to an exposure of 500 kt yr, and we show results assuming high and low resolutions. The horizontal thin lines correspond to the $\Delta\chi^2$ for $\Delta m_{21}^2 = 0$. For NOvA we assume 3 yr nominal exposure for neutrinos as well as anti-neutrinos.

while for larger values the additional information from atmospheric have a larger impact.

4 On the size of Δm_{21}^2 effects in INO

For our simulations of INO data we neglect effects of Δm_{21}^2 . Oscillations of atmospheric neutrinos due to the solar mass-squared difference are important for neutrino energies below 1 GeV, and since we always impose a threshold of 2 GeV Δm_{21}^2 effects are expected to be small. The approximation $\Delta m_{21}^2 = 0$ greatly simplifies the numerical calculations and makes the detailed analysis including parameter correlations, detector resolutions, as well as systematical uncertainties feasible. In this section we check the accuracy of this approximation by considering a simplified analysis taking into account full three-flavour oscillation probabilities.

We consider only statistical errors corresponding to a 500 kt yr INO exposure and neglect systematical uncertainties in the fit. We simulate “data” assuming normal mass ordering, $\sin^2 2\theta_{13} = 0.09$, and $\delta = 0$. Those “data” are fitted with inverted mass ordering, where we keep $|\Delta m_{\text{eff}}^2|$ constant according to Eq. 4. All other oscillation parameters are fixed at the values assumed in generating the data, except for the CP phase δ . The $\Delta\chi^2$ is shown in fig. 8 for low and high resolutions in INO. We see that χ^2 changes by about one

unit as a function of δ . In the figure we also show the $\Delta\chi^2$ value obtained by assuming $\Delta m_{21}^2 = 0$. We conclude that full three-flavour effects do not lead to additional sensitivity to the mass ordering, but will diminish the sensitivity by less than one unit in χ^2 when marginalized over δ . This is true for both assumptions on the resolution. In this sense our INO sensitivities are slightly optimistic. One can expect that those results hold also in the presence of systematical effects.

The various assumptions we had to make at the current stage on reconstruction capabilities and efficiencies introduce uncertainties on the sensitivity which are most likely larger than the one from neglecting the solar mass-splitting, justifying our approximation. However, we stress that once reliable detector properties become available it will be necessary to include full three flavour effects in order to obtain accurate sensitivity predictions.

In Fig. 8 we show also the δ dependence of the χ^2 from NOvA data for the same type of analysis. We see that for NOvA three-flavour effects are essential and there is a significant dependence on the CP phase δ .² Comparing the variation of INO and NOvA we conclude that there is very little complementarity with respect to δ dependent effects. The δ best fit point will be completely dominated by NOvA, and hence the small decrease in sensitivity for INO might be somewhat lifted once combined with NOvA. This results in χ^2 values very similar to the one obtained in the approximation $\Delta m_{21}^2 = 0$.

5 Conclusions

The recent discovery of a relatively large value of θ_{13} by the Daya Bay reactor experiment opens exciting possibilities for the future neutrino oscillation program. In this paper we have focused on the determination of the neutrino mass ordering being normal, $\Delta m_{31}^2 > 0$, or inverted, $\Delta m_{31}^2 < 0$. Currently planned long-baseline accelerator experiments, in particular NOvA and T2K, only have a poor sensitivity to the mass ordering even in case of large θ_{13} . On the other hand, a large θ_{13} provides potentially interesting opportunities for the INO atmospheric neutrino experiment, which is planning to start data taking in 2017. We have investigated the combined sensitivity of these experiments for different assumptions on the size and event reconstruction capabilities of INO.

Assuming “low” resolutions (15% and 15° reconstruction accuracy in neutrino energy and direction, respectively) and a 50 kt detector (fiducial) only a poor global sensitivity is obtained and there is only marginal improvement from combining INO with NOvA and T2K data. Significant synergy and improved sensitivity is obtained for “high” resolution (10% and 10°) and/or doubling the INO detector mass. We find that improving the resolution is more effective than increasing the detector mass. For high resolution we find that a 2σ determination of the mass ordering is possible irrespective of the CP phase δ

²The NOvA curve in Fig. 8 depends strongly on the true value of δ , whereas the result for INO depends only weakly on the assumed value.

in 2021 (2019) with a 50 kt (100 kt) detector. The high resolution 100 kt detector even allows a determination at 3σ around 2025. These conclusions hold for $\sin^2 2\theta_{13} = 0.09$, close to the current best fit point. The sensitivity of the considered experiments still depends crucially on the actual true value of θ_{13} within the currently allowed 3σ region, and to a lesser extent also on θ_{23} .

In our analysis of simulated INO data we assumed a constant efficiency of 85%, and energy and direction resolutions to be independent of energy and direction. These are simplifying assumptions and once a detailed detector simulation becomes available a more realistic analysis should be carried out. We have also discussed the impact of effects related to the solar-mass splitting Δm_{21}^2 and the CP phase δ for the atmospheric neutrino data and have shown that their impact on the sensitivity to the mass ordering is small.

In conclusion, the by now established large value of θ_{13} opens the possibility to determine the neutrino mass ordering within a time frame of about ten years with experiments currently under construction. Atmospheric neutrino data from INO may be crucial in order to achieve this goal and we believe that it is important to include such synergies in the global context towards future neutrino oscillation facilities. Our study suggest, however, that in order to achieve a relevant sensitivity some improvements of the INO detector (either in event reconstruction capabilities, detector mass, or both) seem to be necessary. Complementary information could be provided by e -like events, and the sensitivity of INO could be potentially increased significantly if the reconstruction of charge-separated e -like events was possible [40].

Acknowledgement. We thank Tarak Thakore, Nita Sinha, and Enrique Fernandez-Martinez for useful discussions and Anselmo Meregaglia for spotting a typo in Eq. 4 in earlier versions of this paper.

References

- [1] Super-Kamiokande, Y. Fukuda *et al.*, *Evidence for oscillation of atmospheric neutrinos*, Phys. Rev. Lett. **81**, 1562 (1998), hep-ex/9807003.
- [2] SNO, Q. R. Ahmad *et al.*, *Direct evidence for neutrino flavor transformation from neutral-current interactions in the Sudbury Neutrino Observatory*, Phys. Rev. Lett. **89**, 011301 (2002), nucl-ex/0204008.
- [3] CHOOZ Collaboration, M. Apollonio *et al.*, *Search for neutrino oscillations on a long baseline at the CHOOZ nuclear power station*, Eur.Phys.J. **C27**, 331 (2003), hep-ex/0301017.
- [4] KamLAND, T. Araki *et al.*, *Measurement of neutrino oscillation with KamLAND: Evidence of spectral distortion*, Phys. Rev. Lett. **94**, 081801 (2005), hep-ex/0406035.
- [5] MINOS, P. Adamson *et al.*, *Measurement of Neutrino Oscillations with the MINOS Detectors in the NuMI Beam*, Phys. Rev. Lett. **101**, 131802 (2008), 0806.2237.

- [6] T. Schwetz, M. Tortola, and J. W. F. Valle, *Global neutrino data and recent reactor fluxes: status of three-flavour oscillation parameters*, New J. Phys. **13**, 063004 (2011), 1103.0734.
- [7] T. Schwetz, M. Tortola, and J. W. F. Valle, *Where we are on θ_{13} : addendum to 'Global neutrino data and recent reactor fluxes: status of three- flavour oscillation parameters'*, New J. Phys. **13**, 109401 (2011), 1108.1376.
- [8] L. Wolfenstein, *Neutrino Oscillations in Matter*, Phys.Rev. **D17**, 2369 (1978).
- [9] V. D. Barger, K. Whisnant, S. Pakvasa, and R. Phillips, *Matter Effects on Three-Neutrino Oscillations*, Phys.Rev. **D22**, 2718 (1980).
- [10] S. Mikheev and A. Smirnov, *Resonance Amplification of Oscillations in Matter and Spectroscopy of Solar Neutrinos*, Sov.J.Nucl.Phys. **42**, 913 (1985).
- [11] H. Minakata and H. Nunokawa, *Exploring neutrino mixing with low energy super-beams*, JHEP **10**, 001 (2001), hep-ph/0108085.
- [12] V. Barger, D. Marfatia, and K. Whisnant, *Breaking eight-fold degeneracies in neutrino CP violation, mixing, and mass hierarchy*, Phys. Rev. **D65**, 073023 (2002), hep-ph/0112119.
- [13] DAYA-BAY Collaboration, F. An *et al.*, *Observation of electron-antineutrino disappearance at Daya Bay*, Phys.Rev.Lett. **108**, 171803 (2012), 1203.1669.
- [14] RENO collaboration, J. Ahn *et al.*, *Observation of Reactor Electron Antineutrino Disappearance in the RENO Experiment*, Phys.Rev.Lett. **108**, 191802 (2012), 1204.0626.
- [15] T2K, K. Abe *et al.*, *Indication of Electron Neutrino Appearance from an Accelerator-produced Off-axis Muon Neutrino Beam*, Phys. Rev. Lett. **107**, 041801 (2011), 1106.2822.
- [16] DOUBLE-CHOOZ Collaboration, Y. Abe *et al.*, *Indication for the disappearance of reactor electron antineutrinos in the Double Chooz experiment*, Phys.Rev.Lett. **108**, 131801 (2012), 1112.6353.
- [17] T2K, Y. Itow *et al.*, *The JHF-Kamioka neutrino project*, (2001), hep-ex/0106019.
- [18] NOvA Collaboration, D. Ayres *et al.*, *NOvA: Proposal to build a 30 kiloton off-axis detector to study $\nu_\mu \rightarrow \nu_e$ oscillations in the NuMI beamline*, (2004), hep-ex/0503053.
- [19] DoubleChooz, F. Ardellier *et al.*, *Double Chooz: A search for the neutrino mixing angle θ_{13}* , (2006), hep-ex/0606025.
- [20] RENO, J. K. Ahn *et al.*, *RENO: An Experiment for Neutrino Oscillation Parameter θ_{13} Using Reactor Neutrinos at Yonggwang*, (2010), 1003.1391.
- [21] Daya-Bay, X. Guo *et al.*, *A precision measurement of the neutrino mixing angle θ_{13} using reactor antineutrinos at Daya Bay*, (2007), hep-ex/0701029.

- [22] M. Mezzetto and T. Schwetz, θ_{13} : *phenomenology, present status and prospect*, J. Phys. **G37**, 103001 (2010), 1003.5800.
- [23] P. Huber, M. Lindner, T. Schwetz, and W. Winter, *First hint for CP violation in neutrino oscillations from upcoming superbeam and reactor experiments*, JHEP **11**, 044 (2009), 0907.1896.
- [24] P. Huber, M. Lindner, and W. Winter, *Synergies between the first generation JHF-SK and NuMI superbeam experiments*, Nucl.Phys. **B654**, 3 (2003), hep-ph/0211300.
- [25] H. Minakata, H. Nunokawa, and S. J. Parke, *The Complementarity of eastern and western hemisphere long baseline neutrino oscillation experiments*, Phys.Rev. **D68**, 013010 (2003), hep-ph/0301210.
- [26] S. Prakash, S. K. Raut, and S. Sankar, *Getting the best out of T2K and NOvA*, (2012), 1201.6485.
- [27] INO, India-Based Neutrino Observatory, <http://www.ino.tifr.res.in/ino/>
- [28] N. Mondal, India-Based Neutrino Observatory, Talk at Lepton-Photon 2011, TIFR, Mumbai, India, <http://www.tifr.res.in/~lp11/>, 2011.
- [29] MINOS Collaboration, P. Adamson *et al.*, *First observations of separated atmospheric $\nu(\mu)$ and anti- $\nu(\mu)$ events in the MINOS detector*, Phys.Rev. **D73**, 072002 (2006), hep-ex/0512036.
- [30] MINOS Collaboration, P. Adamson *et al.*, *Charge-separated atmospheric neutrino-induced muons in the MINOS far detector*, Phys.Rev. **D75**, 092003 (2007), hep-ex/0701045.
- [31] S. Petcov, *Diffraction - like (or parametric resonance - like?) enhancement of the earth (day - night) effect for solar neutrinos crossing the earth core*, Phys.Lett. **B434**, 321 (1998), hep-ph/9805262.
- [32] E. K. Akhmedov, A. Dighe, P. Lipari, and A. Y. Smirnov, *Atmospheric neutrinos at Super-Kamiokande and parametric resonance in neutrino oscillations*, Nucl. Phys. **B542**, 3 (1999), hep-ph/9808270.
- [33] M. Chizhov, M. Maris, and S. T. Petcov, *On the oscillation length resonance in the transitions of solar and atmospheric neutrinos crossing the earth core*, (1998), hep-ph/9810501.
- [34] M. Chizhov and S. Petcov, *New conditions for a total neutrino conversion in a medium*, Phys.Rev.Lett. **83**, 1096 (1999), hep-ph/9903399.
- [35] E. K. Akhmedov, M. Maltoni, and A. Y. Smirnov, *1-3 leptonic mixing and the neutrino oscillograms of the Earth*, JHEP **0705**, 077 (2007), hep-ph/0612285.
- [36] T. Tabarelli de Fatis, *Prospects of measuring $\sin^2 2\theta_{13}$ and the sign of Δm^2 with a massive magnetized detector for atmospheric neutrinos*, Eur.Phys.J. **C24**, 43 (2002), hep-ph/0202232.

- [37] J. Bernabeu, S. Palomares Ruiz, and S. Petcov, *Atmospheric neutrino oscillations, $\theta(13)$ and neutrino mass hierarchy*, Nucl.Phys. **B669**, 255 (2003), hep-ph/0305152.
- [38] S. Palomares-Ruiz and S. Petcov, *Three-neutrino oscillations of atmospheric neutrinos, $\theta(13)$, neutrino mass hierarchy and iron magnetized detectors*, Nucl.Phys. **B712**, 392 (2005), hep-ph/0406096.
- [39] D. Indumathi and M. Murthy, *A Question of hierarchy: Matter effects with atmospheric neutrinos and anti-neutrinos*, Phys.Rev. **D71**, 013001 (2005), hep-ph/0407336.
- [40] S. Petcov and T. Schwetz, *Determining the neutrino mass hierarchy with atmospheric neutrinos*, Nucl.Phys. **B740**, 1 (2006), hep-ph/0511277.
- [41] A. Samanta, *The Mass hierarchy with atmospheric neutrinos at INO*, Phys.Lett. **B673**, 37 (2009), hep-ph/0610196.
- [42] J. Kopp and M. Lindner, *Detecting atmospheric neutrino oscillations in the ATLAS detector at CERN*, Phys. Rev. **D76**, 093003 (2007), 0705.2595.
- [43] R. Gandhi *et al.*, *Mass Hierarchy Determination via future Atmospheric Neutrino Detectors*, Phys. Rev. **D76**, 073012 (2007), 0707.1723.
- [44] A. Samanta, *A comparison of the ways of resolving mass hierarchy with atmospheric neutrinos*, Phys. Rev. **D81**, 037302 (2010), 0907.3540.
- [45] T. Kajita, *Mega-ton water Cherenkov detectors for particle and astro- particle physics*, Nucl. Phys. Proc. Suppl. **155**, 87 (2006).
- [46] G. Fogli, E. Lisi, A. Marrone, and A. Palazzo, *Global analysis of three-flavor neutrino masses and mixings*, Prog.Part.Nucl.Phys. **57**, 742 (2006), hep-ph/0506083.
- [47] P. Huber, M. Maltoni, and T. Schwetz, *Resolving parameter degeneracies in long-baseline experiments by atmospheric neutrino data*, Phys.Rev. **D71**, 053006 (2005), hep-ph/0501037.
- [48] J.-E. Campagne, M. Maltoni, M. Mezzetto, and T. Schwetz, *Physics potential of the CERN-MEMPHYS neutrino oscillation project*, JHEP **04**, 003 (2007), hep-ph/0603172.
- [49] R. Gandhi, P. Ghoshal, S. Goswami, and S. Uma Sankar, *Resolving the Mass Hierarchy with Atmospheric Neutrinos using a Liquid Argon Detector*, Phys. Rev. **D78**, 073001 (2008), 0807.2759.
- [50] O. Mena, I. Mocioiu, and S. Razzaque, *Neutrino mass hierarchy extraction using atmospheric neutrinos in ice*, Phys. Rev. **D78**, 093003 (2008), 0803.3044.
- [51] K. Abe *et al.*, *Letter of Intent: The Hyper-Kamiokande Experiment — Detector Design and Physics Potential*, (2011), 1109.3262.

- [52] D. Autiero *et al.*, *Large underground, liquid based detectors for astro-particle physics in Europe: Scientific case and prospects*, JCAP **0711**, 011 (2007), 0705.0116.
- [53] H. Nunokawa, S. J. Parke, and R. Zukanovich Funchal, *Another possible way to determine the neutrino mass hierarchy*, Phys. Rev. **D72**, 013009 (2005), hep-ph/0503283.
- [54] A. de Gouvea, J. Jenkins, and B. Kayser, *Neutrino mass hierarchy, vacuum oscillations, and vanishing $|U_{e3}|$* , Phys.Rev. **D71**, 113009 (2005), hep-ph/0503079.
- [55] P. Huber, M. Lindner, and W. Winter, *Simulation of long-baseline neutrino oscillation experiments with GLoBES (General Long Baseline Experiment Simulator)*, Comput.Phys.Commun. **167**, 195 (2005), hep-ph/0407333.
- [56] P. Huber, J. Kopp, M. Lindner, M. Rolinec, and W. Winter, *New features in the simulation of neutrino oscillation experiments with GLoBES 3.0: General Long Baseline Experiment Simulator*, Comput.Phys.Commun. **177**, 432 (2007), hep-ph/0701187.